THE INFLUENCE OF RESIDUAL STRESS ON THE ULTIMATE STRENGTH OF LONGITUDINALLY COMPRESSED STIFFENED PANELS

Shen Li*, Do Kyun Kim**, Simon Benson***

Marine, Offshore and Subsea Technology Group, School of Engineering, Newcastle University, NE1 7RU, Newcastle upon Tyne, United Kingdom

Corresponding authors:

s.li37@newcastle.ac.uk; ** do.kim@newcastle.ac.uk; * simon.benson@newcastle.ac.uk*

ABSTRACT: *Welding-induced residual stress is known to reduce the ultimate compressive strength of moderately slender stiffened panels under longitudinal compression. This paper contributes a quantified measure of this strength reduction and draws some qualitative observations linking the significance of the residual stress influence to the collapse mode of the panel. A series of nonlinear finite element analyses are completed which covers a range of plate slenderness ratios ($\beta = 1.0 - 4.0$) and column slenderness ratios ($\lambda = 0.2 - 1.2$) typical for application to ship structures. Two residual stress scenarios are compared to a baseline stress-free condition. The first scenario includes residual stress in the plate only and the second scenario includes residual stress applied in the plate and the stiffener web. A modified edge function approach, which can be used in combination with a rule-based approach to account for the effects of residual stress, is examined with reference to the numerical results. A significant ultimate strength reduction due to residual stress is found in most test cases. It is found that residual stress in the plate causes a reduction of the ultimate compressive strength of stiffened panels regardless of failure modes. However, the residual stress in the stiffener web dominates the strength reduction of stiffened panels where collapse is triggered by beam-column buckling. Conversely it has little influence on the stiffened panels which collapse in a plate buckling mode. In addition, the modified edge function approach is demonstrated as conservative compared to the present numerical results, with its applicability confined to stocky panels.*

HIGHLIGHTS:

- Numerical collapse test of stiffened panels in compression;
- Significant reduction in ultimate compressive strength due to residual stress;
- The role of residual stress in stiffener is failure mode-dependent;
- Modified edge function approach is practical yet conservative;

KEYWORDS: residual stress; ultimate strength; buckling; stiffened panel; finite element method

NOMENCLATURE

a = Plate length

b = Plate width

h_w = Height of stiffener web

t_w = Thickness of stiffener web

b_f = Width of stiffener flange

t_f = Thickness of stiffener flange

b_t = Width of tensile stress block

σ_{Yp} = Material yield stress of plating

σ_{Yeq} = Equivalent material yield stress of stiffener panel

ε_{Yeq} = Equivalent material yield strain of stiffener panel

E = Young's modulus

β = Plate slenderness ratio

λ = Column slenderness ratio

σ_{rtx} = Tensile residual stress

σ_{rcx} = Compressive residual stress

ΔQ_{max} = Weld heat input

L_w = Weld leg length

w_{opl} = Local plate distortion

w_{oc} = Column-type distortion

w_{os} = Stiffener sideway distortion

σ_{xu} = Ultimate strength of stiffened panel

ε_{xu} = Ultimate strain of stiffened panel

1. INTRODUCTION

Ships and offshore floating structures are usually constructed from moderately slender stiffened panels, and the assessment of their ultimate in-plane compressive strength is a critical step in a limit state design approach. The ultimate strength of a nominal stiffened panel is influenced by several parameters introduced during fabrication including thickness changes, distortions, misalignments, local material property changes and residual stresses. These factors act in combination to cause a moderate level of uncertainty in the prediction of ultimate strength. Residual stress, which is the focus of this paper, is predominantly caused by the heat imparted into the plating along a weld, typically fillet welds of attached stiffeners and butt welds between adjacent plates. The rapid heating of the separate parts and subsequent cooling of the welded construction introduces a tension stress zone close to the weld which is balanced by compressive stress zone away from the weld. It is well established that the residual stress causes a reduction in the ultimate strength. This paper quantifies this as a function of the plate and column slenderness ratio of the panel. Observations of the panel collapse mode are linked to the significance of the residual stress strength reduction.

Several case studies can be found in the literature on the effects of welding-induced residual stress. Gannon et al. [1] conducted a nonlinear collapse analysis on tee-bar and angle-bar stiffened plates under compression considering welding-induced residual stress. A three-dimensional thermo-elastoplastic finite element analysis was carried out to simulate the heat transfer from welding. The results suggested that the ultimate strength of tee-bar stiffened panels may be reduced by 12.5% due to the resulting residual stress. With the same approach, it was reported by Gannon et al. [2] that the reduction in flat-bar stiffened panels was up to 16.5%. Hansen [3] concluded that residual stress may lead to a decrease of ultimate strength by 25%, while Gordo and Guedes Soares [4] found that the ultimate strength was reduced by 10% when the compressive residual stress in the plate was taken as 20% of the yield stress. Khan and Zhang [5] indicated that the ultimate strength reduction of stiffened panels was up to 10% to 13%. Regarding the hull girder strength, it was shown by Gannon et al. [6] that the hull girder strength can be reduced by 3.3% in the case that the ultimate strength of its component stiffened panels was decreased by 11%. The literature survey indicates that the welding-induced residual stress would lead to a reduction of the ultimate compressive strength of stiffened panels.

An efficient modified edge function approach was suggested in [4] and [7] to deal with the effects of residual stress in strength assessment. This may also be employed in combination with the CSR-H approach [8-9], since these two methods are developed in a similar way with a major difference in their effective width model where

the Faulkner formula is applied in the former and Frankland formula is embedded in the latter. A comprehensive examination is necessary to confirm the applicability of this approach.

As an extension to previous work [10], a parametric numerical study is conducted in this paper to assess the effects of welding-induced residual stress on the ultimate compressive strength of stiffened panels. The test matrix covers a wide range of plate slenderness ratios ($\beta = 1.0 \sim 4.0$) and column slenderness ratios ($\lambda = 0.2 \sim 1.2$), typical for ships and ship-type floating structures. While the previous study only considered the residual stress on local plating, two residual stress scenarios are compared to a baseline stress free condition in this work to further reveal the effects of welding residual stress on stiffened panels with different buckling failure modes. In the meantime, the modified edge function approach, employed in combination with the CSR-H method, is examined with reference to the numerical results for evaluating its applicability to account for the effects of residual stress. Additionally, there are a few case studies to analyse the sensitivity of residual stress to various stiffener profiles and to evaluate the relationship between the residual stress magnitudes and stiffened panels with different slenderness.

2. BACKGROUND

2.1 Recent Advancements in ULS Design

The ultimate limit state (ULS) assessment is a principle part of the safety evaluation of marine structures. Recent advancements include the developments of novel methodologies for predicting the ultimate strength of ship hull girders [11-12] and structural components [13-14]. In addition, the understanding in the collapse mechanism of marine structures is much improved attributing to numerous investigations on the ultimate strength performance of stiffened plated ship structures in relation to slenderness [15-19], initial imperfection [20-21], boundary condition [22], secondary loading [23-25], cyclic loading [26-31], arctic environment [32-36], elevated temperature [37], corrosion [38-43], fatigue crack [44] and accidental damage [45-49].

In most of these studies the effects of welding-induced residual stress are omitted. This is likely due to the debate on whether the residual stress effect should be incorporated in the strength assessment of ship structures. It is argued that residual stress of stiffened panels may be partially removed by shakedown, since the ships are subjected to a cyclic loading when in service. However, a recent study by Cerik and Cho [50] on the stiffened cylindrical shell indicated that the cyclic compressive load would not lead to a significant residual stress relief. Moreover, the analysis by Gannon et al. [51] on flat stiffened panel structures suggested that whist the shakedown phenomenon would lead to a stress relief and an increase in the ultimate strength, its mechanism is fairly complex

and is dependent on the failure mode of the panels. Additionally, the reduction in residual stress is not uniform throughout the plate-stiffener combination. Therefore, if the collapse initialises in a region with relatively little stress relief, the change in ultimate strength will be small. Hence, it should not be assumed in a hull girder analysis that residual stresses are reduced uniformly throughout the cross section, or even entirely removed, as this may lead to overly optimistic estimates of hull girder ultimate strength.

2.2 The Residual Stress Mechanism

During the welding process, the welding metal is melted with the mother plates until solidification [52]. Shrinkage of the stiffened panels occurs at the solidified part, which is newly constrained by the surrounding un-melted part. As a result, tensile stress is induced in the solidified part and compressive stress is developed at the neighbouring part to maintain an equilibrium condition (Figure 1). Different welding types are available according to the specific requirements. The scope of this paper is confined to the welding between longitudinal stiffeners and the attached plating with a fillet weld. The welding between two plates is not considered. This may be justified for the fact that the residual stress developed in this case may increase the buckling strength of the panel due to the tensile stress filed developed near the centre of the plating where buckling would take place [53].

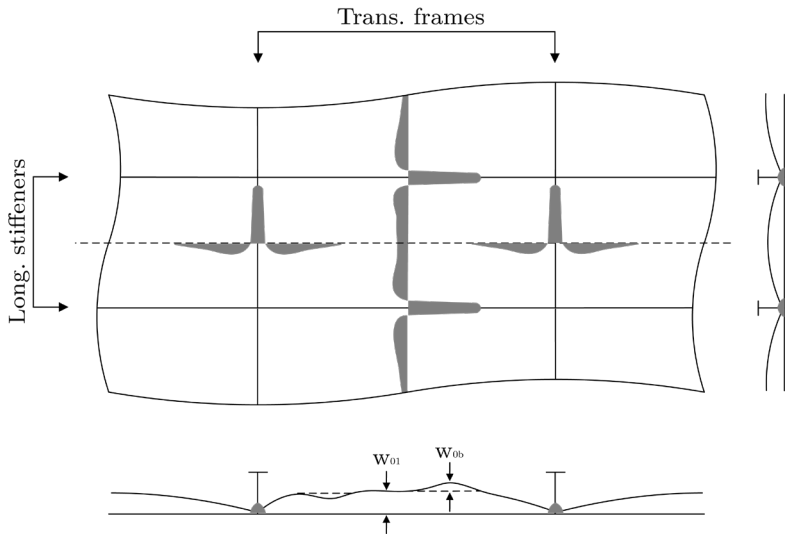

Figure 1. Schematic illustration of initial imperfection caused by welding reproduced from [52]

2.3 Distribution and Magnitude of Residual Stress

Smith et al. [16] suggested a simplified welding-induced residual stress distribution for stiffened panels (Figure 2a), in which the residual stress field was idealised as tension and compression blocks. In addition, a triangular

distribution shape was assumed for the compressive stress field of stiffener's web, while the tensile stress field was taken as a rectangular strip near the intersection with plating. A similar distribution was given by Yao and Fujikubo [52] for fillet welding (Figure 2b). However, a uniform distribution was assumed for the compressive stress field along the height of the stiffener's web. A more elaborated bi-axial distribution pattern for the plating was given by Paik and Thayamballi [54] considering the residual stress in both longitudinal and transverse directions (Figure 2c). The recent full-scale measurements [55-57] and numerical simulation [58] of welding-induced residual stress confirm the rationality of these idealisations of residual stress distributions. Note that there would be a minor deviation between the actual measurement and the simplified rectangular distribution shape. However, this is not expected to cause any significant difference in the ultimate strength of stiffened panels under uniaxial compression.

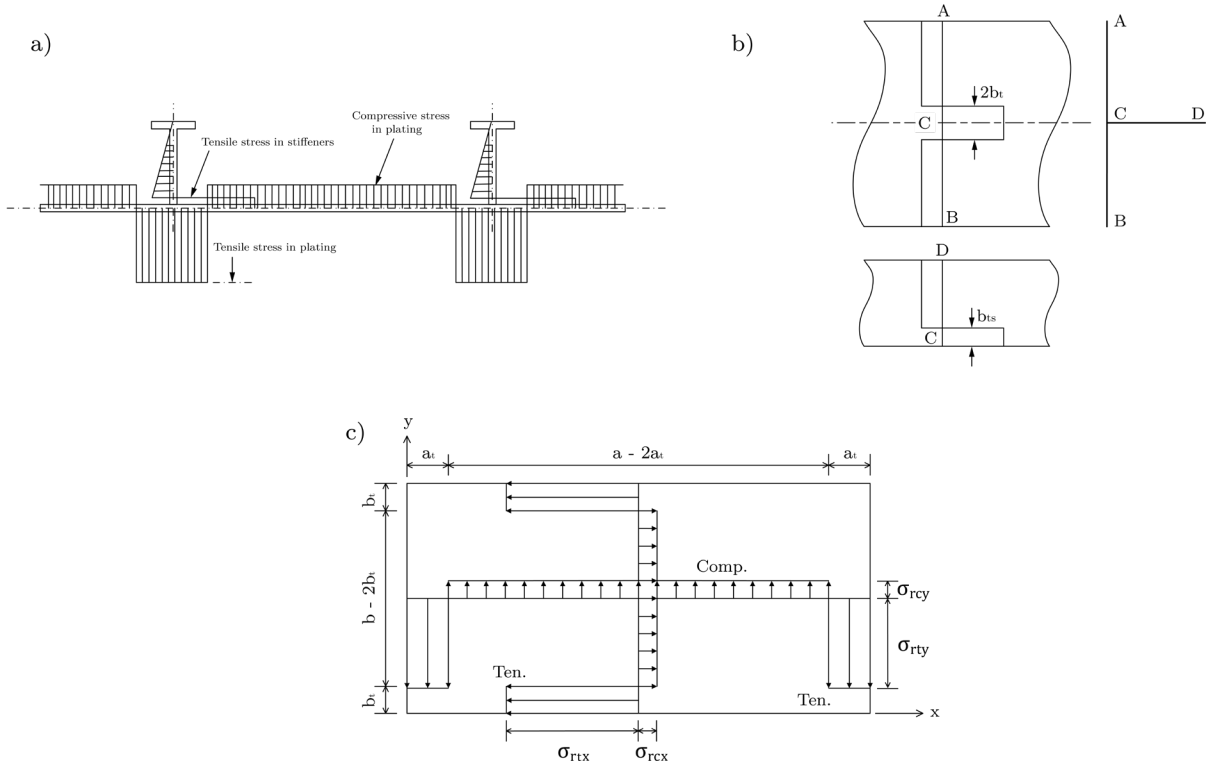

Figure 2. Idealised distribution of the welding-induced residual stress in stiffened panels

Since the residual stress is self-equilibrating, the equilibrium condition gives the relationship of Equation (1) where the total tensile force is equal to the total compressive force.

$$2b_t\sigma_{rtx} = (b - 2b_t)\sigma_{rcx} \tag{1}$$

To determine the magnitude of the residual stress, Yao [59] suggested that the width of the tensile block can be expressed as a function of plating thickness t_p, web thickness t_w and the weld heat input ΔQ_{max} (Equation 2). Meanwhile, the tensile yield stress is equal to the material yield stress in the case of ordinary steel.

$$b_t = t_w/2 + 0.26\Delta\, Q_{max}/\left(t_w + 2t_p\right) \tag{2}$$

Yi et al. [60] developed an empirical formulation to predict the welding-induced residual stress. The breadth of the longitudinal tensile residual stress block is proposed as a function of the plate slenderness ratio β and the weld leg length L_w (Equation 3).

$$b_t = c_1 \times L_w + d_1 \tag{3}$$

where

$$c_1 = -0.6212\beta^2 + 5.9145\beta - 3.3894$$

$$d_1 = 1.9505\beta^2 - 16.234\beta + 18.711$$

An empirical formula was given by Smith et al. [16] to estimate the compressive residual stress. Three different severities, i.e. slight (Equation 4a), average (Equation 4b) and severe (Equation 4c), were proposed.

$$\sigma_{rcx} = 0.05\sigma_{Yp}\ (slight) \tag{4a}$$

$$\sigma_{rcx} = 0.15\sigma_{Yp}\ (average) \tag{4b}$$

$$\sigma_{rcx} = 0.30\sigma_{Yp}\ (severe) \tag{4c}$$

2.4 Modified Edge Function Approach

To account for the effect of residual stress, a modified edge function approach was proposed by Gordo and Guedes Soares [4], as illustrated by Figure 3. In principle, an edge function Φ is employed to simulate the material behaviour. In an initial stress-free condition, a bilinear elastic-perfectly plastic material is usually assumed, and the edge function is expressed by Equation (5). However, when the residual stress is introduced, the material behaviour should be modified as trilinear with a reduced stiffness from $1.0 - \varepsilon_{rcx}/\varepsilon_{Yeq}$ till compressive yielding (Equation 6). It is assumed that the compressive yield strain is universally taken as $\varepsilon^c_{Yeq}/\varepsilon_{Yeq} = 2.0$. This assumption is subjected to an examination in this paper. As introduced in section 1, the Gordo and Guedes Soares method was developed in a similar way as the CSR-H approach. Hence, the modified edge function approach can also be applied in the CSR-H method and this examination also has a significance on improving the CSR-H.

Original edge function for initial stress-free condition

$$\Phi = \varepsilon_x/\varepsilon_{Yeq} \qquad \text{if } \varepsilon_x/\varepsilon_{Yeq} \leq 1.0 \tag{5a}$$

$$\Phi = 1.0 \qquad \text{if } \varepsilon_x/\varepsilon_{Yeq} > 1.0 \tag{5b}$$

Modified edge function accounting for residual stress

$$\Phi = \varepsilon_x/\varepsilon_{Yeq} \qquad \text{if } \varepsilon_x/\varepsilon_{Yeq} \leq 1.0 - \varepsilon_{rcx}/\varepsilon_{Yeq} \tag{6a}$$

$$\Phi = \mathrm{E}_T\left(\varepsilon_x/\varepsilon_{Yeq} - 1.0 + \varepsilon_{rcx}/\varepsilon_{Yeq}\right) + 1.0 - \varepsilon_{rcx}/\varepsilon_{Yeq} \qquad \text{if } 1.0 - \varepsilon_{rcx}/\varepsilon_{Yeq} < \varepsilon_x/\varepsilon_{Yeq} \leq 2.0 \tag{6b}$$

$$\Phi = 1.0 \qquad \text{if } \varepsilon_x/\varepsilon_{Yeq} > 2.0 \tag{6c}$$

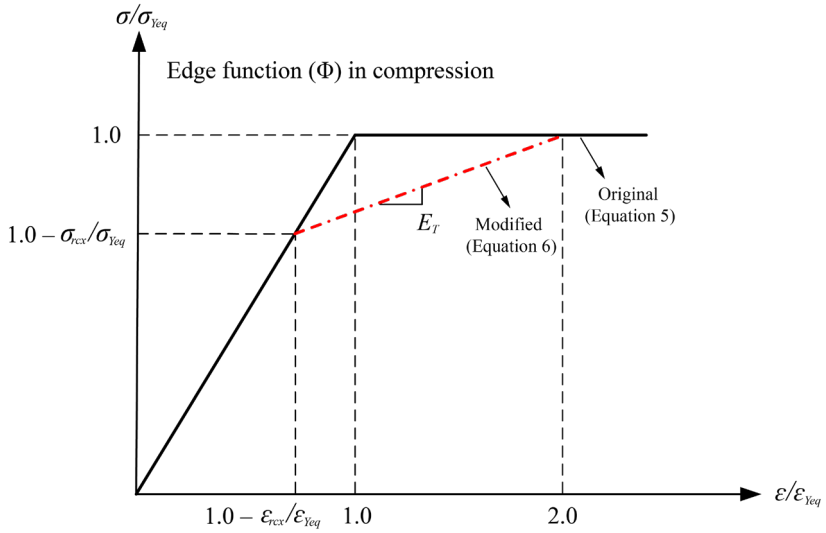

Figure 3. Illustration of the modified edge function to account for the residual stress

3. NUMERICAL CASE STUDY

3.1 Scope of Analysis

To investigate the influence of residual stress on the buckling collapse behaviour, nonlinear finite element analysis is carried out for a series of stiffened panels with three scenarios, namely initial stress-free, residual stress applied only on local plates and residual stress applied on plates and webs. In accordance with the stiffened panel test matrix in [16], the following parameters are varied systematically giving a total of 42 stiffened panels and 42×3=126 test cases in which the notation is defined with reference to Figure 4:

- Plate slenderness ratio: $\beta = b/t_p\sqrt{\sigma_Y/E}$ = 1.0, 1.5, 2.0, 2.5, 3.0, 3.5, 4.0 where b is the plate width, t_p is the plate thickness, σ_Y is the material yield stress of the plate and E is the material Young's modulus.

- Column slenderness ratio: $\lambda = a/\pi r\sqrt{\sigma_{Yeq}/E} = 0.2, 0.4, 0.6, 0.8, 1.0, 1.2$ where a is the length of the panel, r is the radius of gyration, σ_{Yeq} is the equivalent yield stress of the column section and E is the material Young's modulus.
- Stiffener area ratio: $\gamma = A_s/A = 0.2$ where A_s is the cross-sectional area of the stiffener, and A is the total cross-sectional area.
- Stiffener cross-sectional profile: all calculations refer to tee-bar stringers, which corresponds to the 114mm × 44.5mm Admiralty long-stalk tee bar section and is a standard stiffener type used in most of the British naval ships [61].
- Material property: the yield strength and Young's modulus in all calculations are 324MPa and 207000MPa respectively, which is nominal properties for high tensile steel. Elastic-perfectly plastic behaviour is assumed.

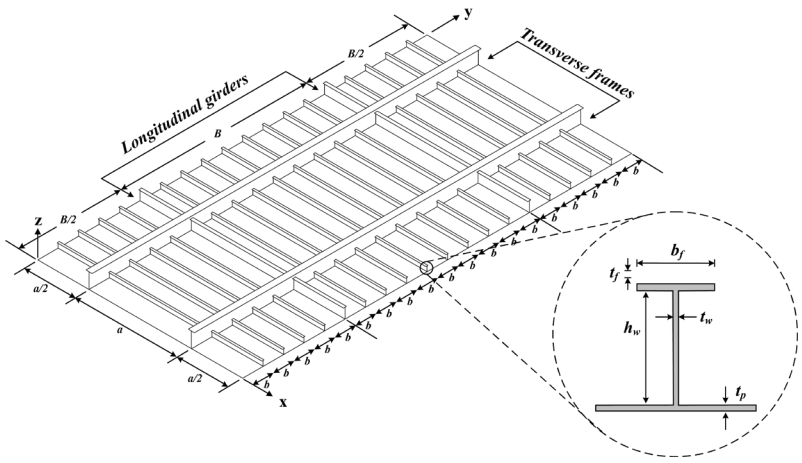

Figure 4. Schematic view of a stiffened panel and dimension notations

The test matrix represents a relatively large spectrum of structural scantlings and covers the most common configurations in the design of primary ship structures. A summary of the scantling of the tested stiffened panel is given in the appendix (Table A1). Dow [62] recommended that the column slenderness ratio of the primary deck and bottom panels should generally be less than 0.45 and should not exceed 0.55. According to a survey by Zhang and Khan [63], the typical plate slenderness ratio and column slenderness ratio of merchant ship structures are in the range of 1.5 to 2.5 and 0.2 to 0.8 respectively. It was indicated in [16] that the stiffener area ratio γ of 0.2 is a common case based on the measurement of naval ships. The test matrix adopted by ISSC [64] suggested that the area ratio is around 0.1 to 0.6 for merchant ship structures. However, as shown in [65], the effect of area

ratio is much less significant than the other two dimensionless parameters (β and λ). Hence, only one stiffener area ratio γ is selected in the present test matrix.

3.2 Initial Imperfection

3.2.1 Initial Distortion

The overall initial distortion field of a stiffened panel is decomposed into three types, including local plate distortion w_{opl}, column-type distortion w_{oc} and stiffener sideway distortion w_{os}, as defined by Equation (7) and schematically shown in Figure 5. The local plate distortion follows the critical buckling mode with "m" sinusoidal half-waves. The number of sinusoidal half -wave is determined by plating aspect ratio (Equation 7d). The column-type distortion and stiffener sideway distortion are both of a single sinusoidal half wave form. The distortion magnitudes are all assumed as an average severity level based on the statistics of imperfection measurement on ship panels (Equation 8). The local plate distortion magnitude is derived as a function of the plate slenderness ratio and plate thickness. The column-type distortion and stiffener sideway distortion magnitudes are both expressed as a function of the panel's length. This definition of the initial distortion is consistent with [64]. There are different definitions of the local plate distortion magnitude in the literature, such as [66-69] where the distortion magnitude was expressed as a function of plate width or a combination of plate width and plate thickness. However, some of these expressions were dedicated to civil engineering structures and may not be applicable in ship structures due to the difference in manufacturing practice and standard. On the contrary, the Equation (8) was developed based on the measurement on ship structures and more importantly it is compatible with Equation (4) for defining the magnitude of residual stress which is used in this study, since they were introduced by the same research group.

$$w_{opl} = A_o sin\left(\frac{m\pi x}{a}\right) sin\left(\frac{\pi y}{b}\right) \text{ (local plate distortion)} \tag{7a}$$

$$w_{oc} = B_o sin\left(\frac{\pi x}{a}\right) sin\left(\frac{\pi y}{B}\right) \text{ (column-type distortion)} \tag{7b}$$

$$w_{os} = C_o \frac{z}{h_w} sin\left(\frac{\pi x}{a}\right) \text{ (stiffener sideway distortion)} \tag{7c}$$

$$a/b \leq \sqrt{m(m+1)} \tag{7d}$$

$$A_o = 0.1\beta^2 t \tag{8a}$$

$$B_o = 0.0015a \tag{8b}$$

$$C_o = 0.0015a \tag{8c}$$

In terms of the relative magnitude between adjacent panels, such as the local plate distortion between adjacent plating, an asymmetric distortion pattern is assumed in this paper. The effect of the relative magnitude between adjacent panels was investigated in [15]. It was shown that a symmetric pattern would increase the ultimate strength whereas an asymmetric pattern will produce a conservative prediction. This is because the former pattern effectively increases the rotational constraints of the panel edges, whereas the latter pattern effectively corresponds to a simply supported boundary. To deal with the effect of relative magnitude, the effective imperfection concept proposed by the Merrison Committee [70] can be referred to. In this paper, it was found that convergence issue may encounter in the nonlinear finite element analysis, when adopting a symmetric distortion pattern in combination with initial residual stress. Hence, for the sake of obtaining reliable FE solutions, the asymmetric distortion pattern is employed.

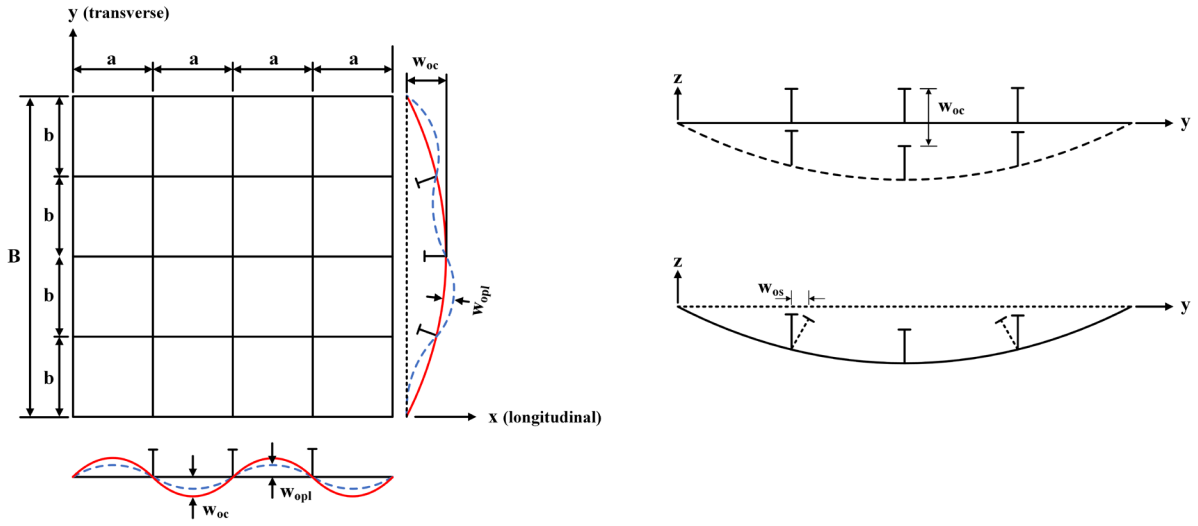

Figure 5. Schematic view of the initial distortions

3.2.2 Initial Residual Stress

Regarding the residual stress, the longitudinal distribution of Figure 2(c) is followed for the attached plates. The width of tensile stress block b_t is determined by assuming that the tensile residual stress equals the material yield stress and the compressive residual stress corresponds the average-level magnitude as given by Equation (3). The residual stress in the transverse direction is ignored, since the ultimate strength performance in longitudinal compression is of concern in this study. The residual stress in stiffeners follows the rectangular distribution pattern of Figure 2(b). The ratio between the height of the tensile stress block and the total web height h_t is taken as $h_t/h_w = 1/6$. In other words, the ratio between the height of the compressive stress block h_c and the tensile

stress block h_t is $h_c/h_t = 5$. This is to satisfy the meshing scheme of stiffeners and it may also correspond to the average-level severity.

In addition, to examine the effects of residual stress in longitudinal stiffeners, the analyses are conducted for all panels with and without residual stress applied on longitudinal stiffeners. The more realistic triangular distribution of stiffener's residual stress is simplified in this study mainly due to the fact that an extra fine mesh may be needed to accurately represent the triangular distribution. The computational effort will thus be significantly increased and likely causes a FE convergence issue. The examination of the effect of stiffener's residual stress will provide insights on whether a future study is required to investigate the influence of different residual stress distribution shapes of longitudinal stiffeners.

3.3 Finite Element Modelling

Two-bays/two-spans model with eight identical stiffeners in each span is employed (Figure 6). This model extent allows for the end-rotation of stiffeners, which may prevent an overestimation of ultimate compressive strength. In the meantime, the interaction between the adjacent structures can be accounted for, following the recommendation by Smith et al. [16]. The longitudinal girder and transverse frame are modelled with boundary condition constraining the out-of-plane movement. The present model may be a reasonable representation of typical continuous ship grillages shown by the benchmark study in [64]. The boundary conditions and the number of stiffeners at each span would affect the ultimate strength characteristics of stiffened panels. However, these are out of the scope of this study, the effects of which were investigated by Xu et al. [22] and Tanaka et al. [19] respectively.

The FE model is discretised with four-node shell element with reduced integration (S4R in ABAQUS), which is consistent with [12-14]. For the local plating, the element number in the longitudinal direction is dependent on the column slenderness ratio as 50λ. Conversely, ten elements are universally employed in the transverse direction for all cases, including one element at each boundary for the tensile residual stress block and eight equal size elements for the central compressive stress block, which gives a characteristic plating mesh size of 50mm × 50mm. For the stiffeners, six elements are used in both stiffener's web and flange.

The initial imperfection is defined by an external subroutine, in which the initial distortion is applied using a direct-node translation technique and the welding-induced residual stress is modelled by defining the initial stress of each element [71]. A relaxation step prior to any other external load application is utilised for the self-equilibrium of the initial stress field. It should be noted that the relaxation step would lead to a minor difference

on the geometric imperfection. However, the difference would be negligible, usually less than 0.5mm. The relaxation step aims to achieve a self-equilibrium of the applied stress field, which in some cases could help avoiding the convergence issue of obtaining numerical solution. The modelling approach of residual stress is consistent with studies presented in [15-16]. An example FE model after the residual stress relaxation is shown in Figure 7. The primary purpose of this paper is to investigate the strength reduction caused by welding residual stress. With the present modelling, the reduction is in generally of a similar magnitude as compared with the study in [1], which may verify the validity of the adopted modelling approach.

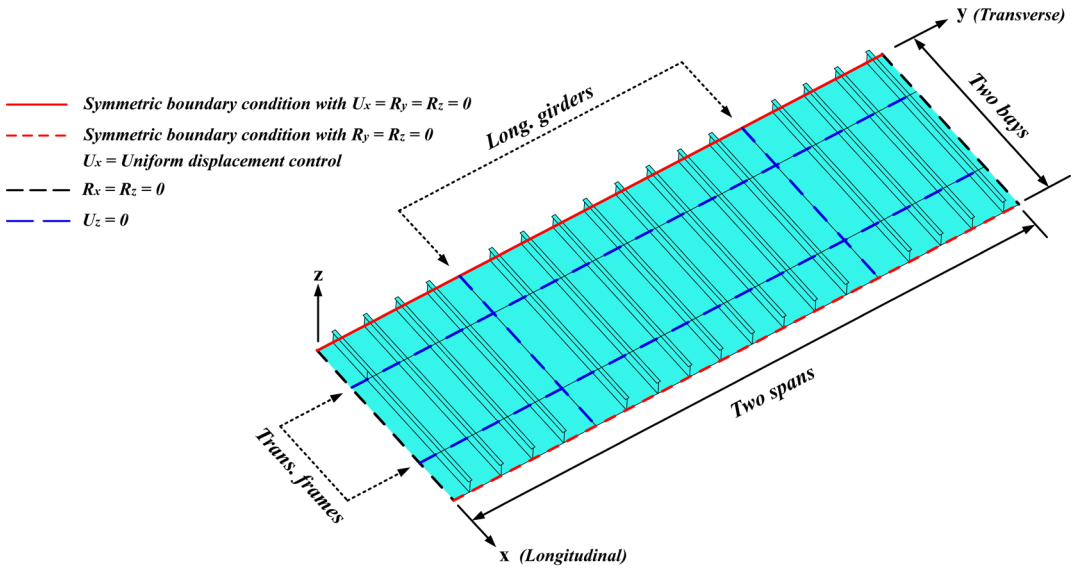

Figure 6. The boundary conditions of the FE model

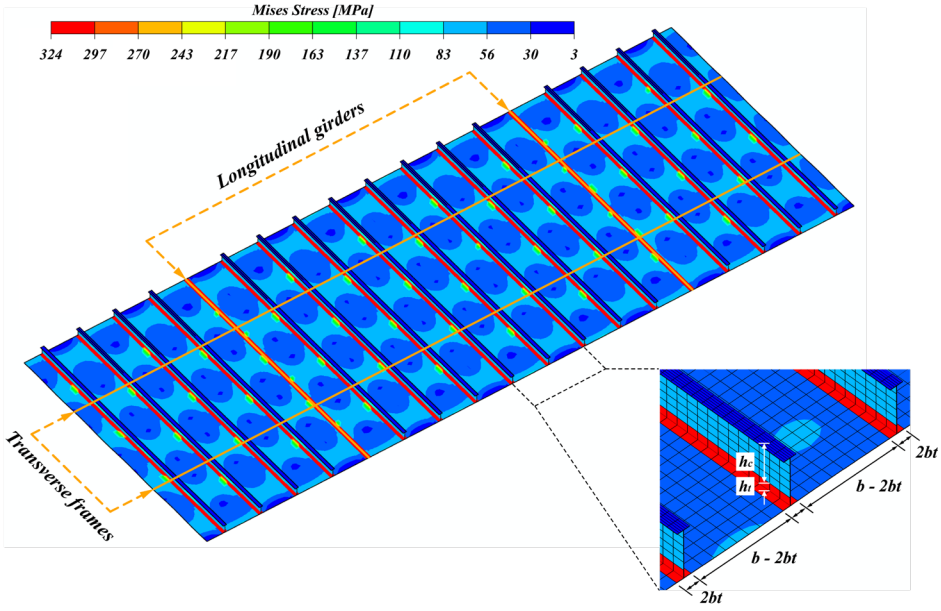

Figure 7. Stiffened panel after relaxation of the initial residual stress

3.4 Results and Discussions

3.4.1 Validation of Nonlinear FEM Results

To validate the NLFEM results, a comparison on the calculated ultimate compressive strength by initial stress-free NLFEM with three empirical formulae and IACS-CSR is shown in Figure 8. The empirical formulae refer to Paik and Thayamballi [72], Zhang and Khan [63] and Kim et al. [73]. The P-T formula was developed from experimental measurements. Hence, both initial distortion and welding-induced residual stress were implicitly included. Z-K formula [63] and Kim formula [73] were proposed on the basis of ABAQUS and ANSYS finite element solutions respectively, both of which excluded the effect of welding-induced residual stress. In addition, the deflection magnitudes were also different. For the local plate deflection, Z-K formula is embedded with the Dowling's recommendation, whereas Kim formula follows Smith's recommendation [16], i.e. $w_{max} = b/200$ and $w_{max} = 0.1\beta^2 t$ respectively. Comprehensive reviews of these empirical formulations can be found in [74-75].

Apart from comparing on the whole spectrum, the comparison is also performed for four sub-domains as suggested in [76], namely sub-domain 1 ($\beta > 1.9$ & $\lambda \leq 0.6$), sub-domain 2 ($\beta > 1.9$ & $\lambda > 0.6$), sub-domain 3 ($\beta \leq 1.9$ & $\lambda \leq 0.6$) and sub-domain 4 ($\beta \leq 1.9$ & $\lambda > 0.6$). The subdivision of four sub-domains is based on von-Karman formula and the study by Ozdemir et al. [77]. The former indicates that the compressive strength of plating may change substantially when $\beta > 1.9$, while the latter suggests that the primary failure mode of stiffened panels under compression may change from local plate buckling to beam–column buckling at the threshold $\lambda = 0.6$. The purpose of a domain subdivision is to better provide insights into the ultimate strength performance of stiffened panel dominated by different buckling failure modes.

A closer correlation is obtained with the P – T formula and Kim formula, whereas the present NLFEM results are conservative as compared with Z – K formula and CSR-H. The discrepancy is mainly driven by to the difference in imperfection characteristics. For instance, P – K formula was developed from as-built imperfection while Z – K formula and Kim formula were based on idealised shapes. In addition, the model extent may be another contributor. The present NLFEM model is consistent with that used in the development of Kim formula, whereas Z – K formula was developed from a smaller model extent. The present NLFEM results may be concluded as reasonable. More importantly, the emphasis in this paper is placed on the strength reduction due to residual stress, which should be weakly dependent on the uncertainty factors such as imperfection characteristics and model extent.

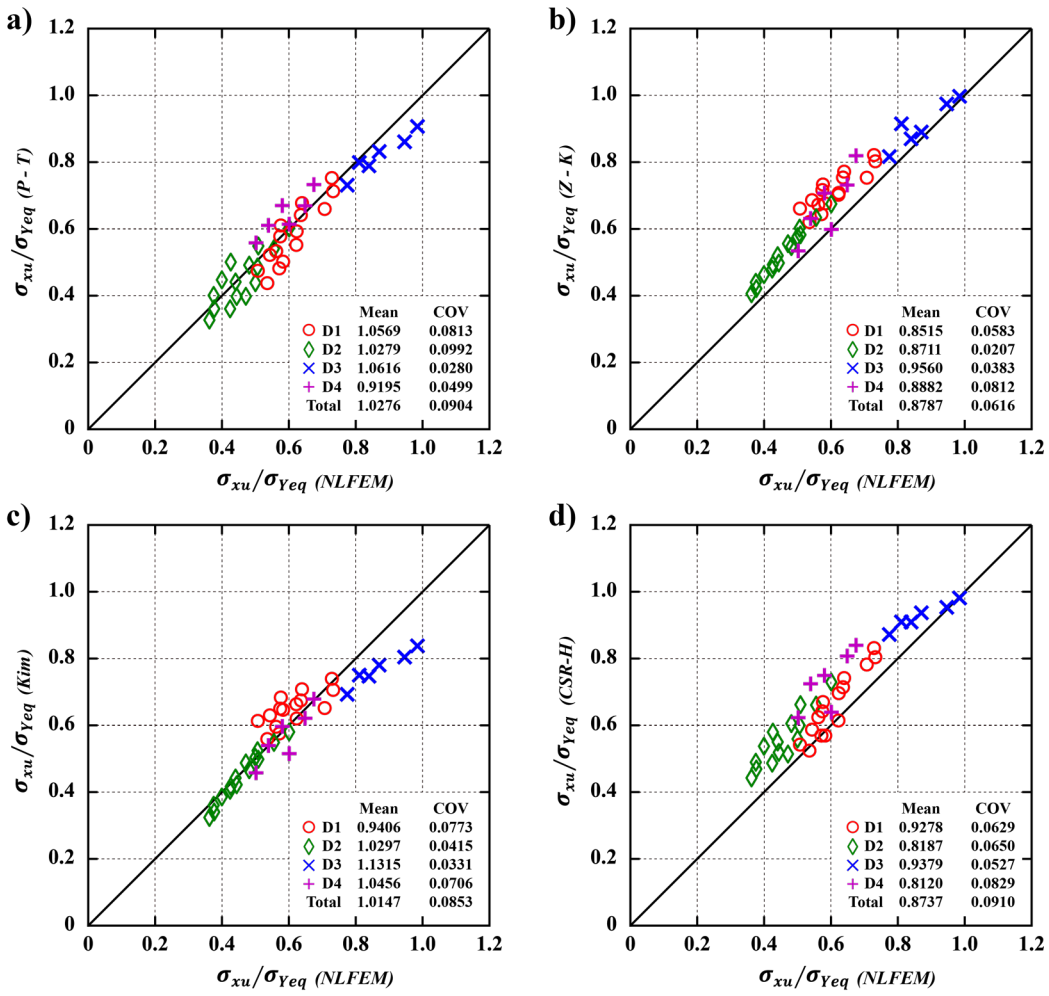

Figure 8. Comparison with various formulae: a) Paik-Thayamballi; b) Zhang and Khan; c) Kim et al.; d) CSR-H.

Note: D1 = $\beta > 1.9$ & $\lambda \leq 0.6$; D2 = $\beta > 1.9$ & $\lambda > 0.6$; D3 = $\beta \leq 1.9$ & $\lambda \leq 0.6$; D4 = $\beta \leq 1.9$ & $\lambda > 0.6$

3.4.2 Ultimate Compressive Strength Reduction

In this section, the ultimate compressive reduction caused by the initial residual stress is discussed. A cubic interpolated contour plot of the ultimate compressive strength reduction caused by residual stress is shown in Figure 9. Three cases are illustrated in the contour plots, namely NLFEM with residual stress in plate only, NLFEM with residual stress in plate and web and CSR-H with compressive yield strain = 2.0. Note that all failure modes in the CSR-H formulation are considered. As predicted by the NLFEM, a significant ultimate strength reduction is found on most tested panels, except for the combination of low plate slenderness ratio and high column slenderness ratio (sub-domain 4) or the combination of high plate slenderness ratio and low column slenderness ratio (sub-domain 1). In the former case (small β & large λ), the collapse of the stiffened panel is triggered by an inter-frame overall collapse of plate and stiffener as a unit (Figure 10a), which corresponds to the Mode I-1 collapse type for uniaxially stiffened panels as defined by Paik and Thayamballi [54]. In this case, the

stiffener size is small relative to the plating dimension and the ultimate strength is attained when a large yielding zone is formed in the panel without significant local plate buckling. Conversely in the latter case (large β & small λ), the plating dimension is small relative to the stiffeners. Significant tripping (sideway buckling) associated with a widespread yielding zone is found in the stiffeners (Figure 10b). This is likely due to a relatively small torsional rigidity of the overall column because the plating is extremely slender. Hence, in this case, the effect of residual stress on the ultimate compressive strength is minimum, even with its application on the stiffener's web. In terms of the stiffened panels that are substantially affected by the residual stress (sub-domain 2 and 3), their collapse is usually dominated by the local buckling accompanied by a considerable beam-column flexural behaviour (Figure 10c). For stiffened panels in sub-domain 3, the local buckling is the predominant failure mode. For stiffened panels in sub-domain 2, the collapse is governed by the beam-column buckling. In these panels, even with the residual stress applied only in the local plate, a fairly large reduction of the ultimate strength is shown, which would then be increased with a further application in the stiffener's web. However, the prediction by CSR-H based on the modified edge function approach, assuming that compressive yield strain equals to 2.0, is inconsistent with this observation and is much more conservative in most cases.

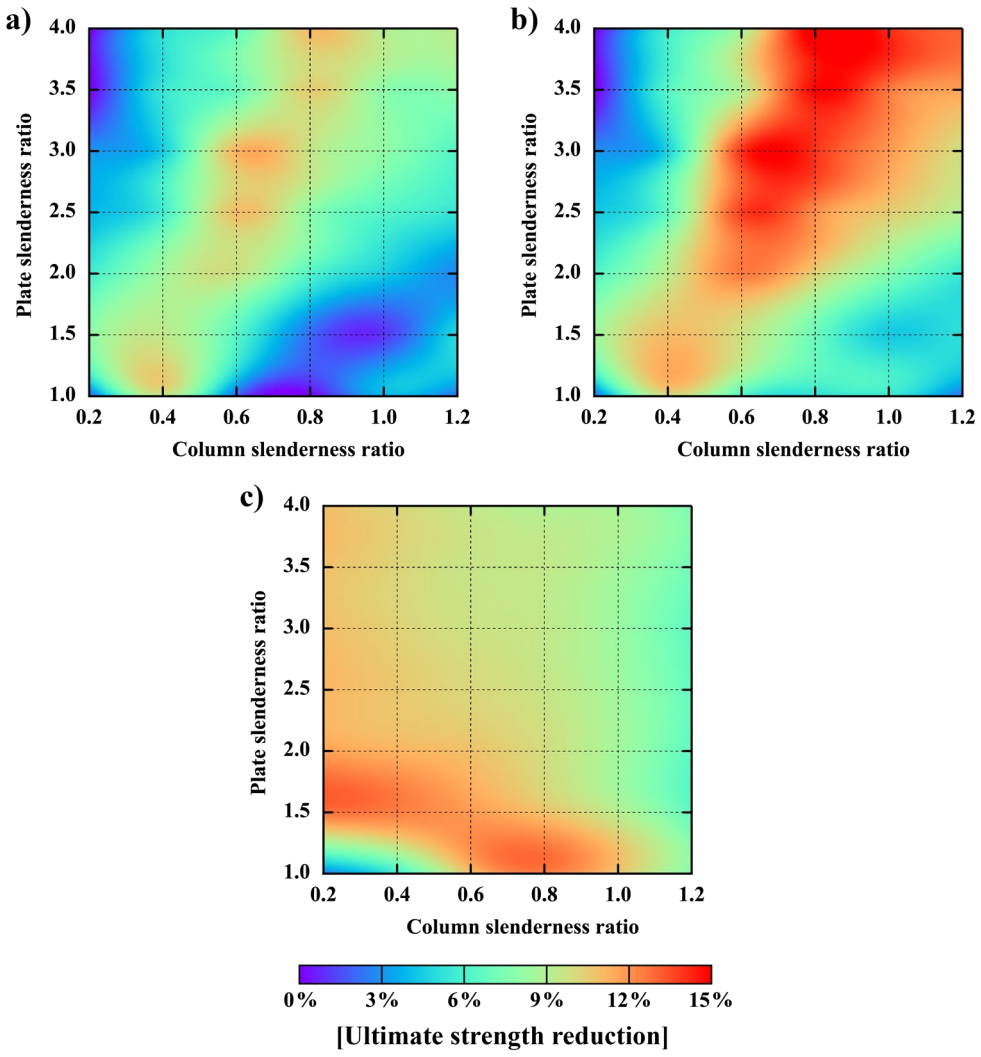

Figure 9. Cubic interpolation contour of the ultimate strength reduction caused by welding residual stress. a) NLFEA (Residual stress in plate only); b) NLFEA (Residual stress in plate and web; c) CSR-H (Compressive yield strain = 2.0)

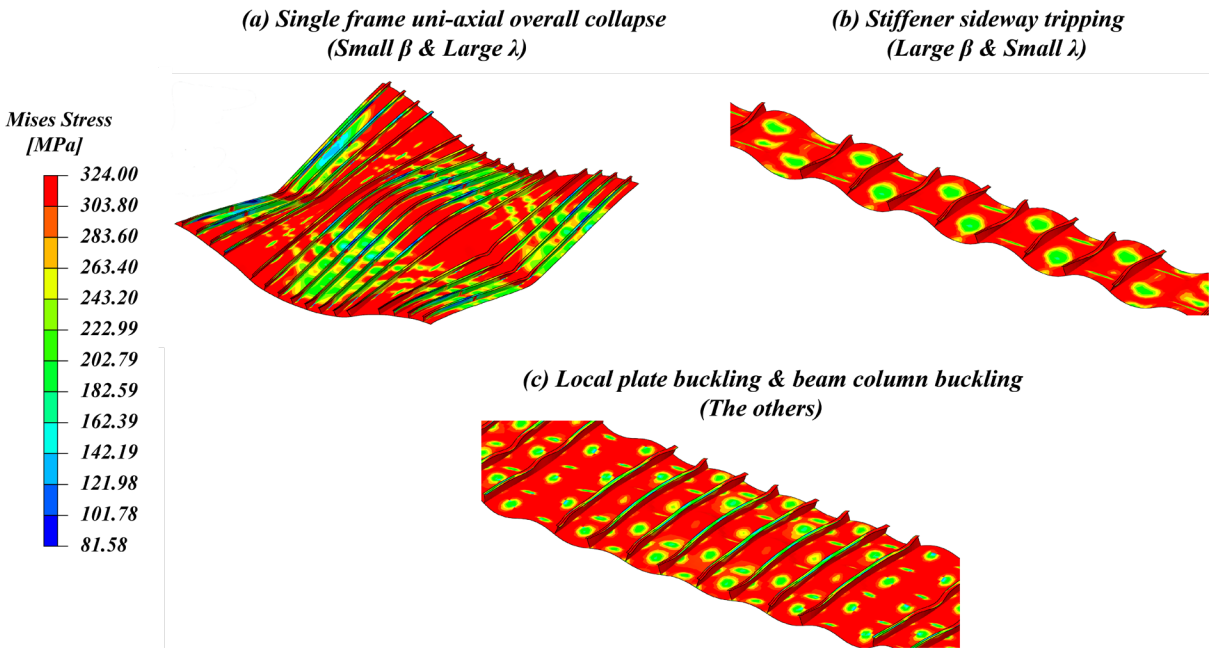

Figure 10. Failure modes of stiffened panels with different combination of plate and column slenderness ratios

Table 1 to Table 3 summarise the prediction of ultimate compressive strength reduction by NLFEM and CSR-H. The prediction discrepancy is further illustrated in Figure 11. According to the NLFEM results, an average reduction of 6.25% is induced by residual stress in local plate only, while an average of 8.71% reduction is resulted by the residual stress in both local plate and stiffener's web. Although only marginal increase is found on panels predominately with local plate failure (sub-domain 3), the residual stress in web may double the strength reduction of stiffened panels predominately with beam-column type failure (sub-domain 2). Hence, it may be concluded that the residual stress in stiffener's web is equally important as compared with the attached plating residual stress. Full-scale measurement should be conducted to investigate its magnitude and distribution. Meanwhile, it can be seen that the CSR-H method is generally overestimated in terms of the strength reduction with an average of 9.46%, in particular for stocky panels with low column slenderness ratio or low plate slenderness ratio.

Table 1. Summary of the ultimate compressive reduction (NLFEM with residual stress in plate only)

	$\lambda = 0.2$	$\lambda = 0.4$	$\lambda = 0.6$	$\lambda = 0.8$	$\lambda = 1.0$	$\lambda = 1.2$
$\beta = 1.0$	2.16%	9.57%	2.10%	0.16%	3.90%	2.33%
$\beta = 1.5$	7.88%	9.38%	6.39%	2.18%	1.04%	4.94%
$\beta = 2.0$	5.82%	8.60%	9.67%	6.24%	4.50%	2.78%
$\beta = 2.5$	3.94%	5.93%	10.89%	7.95%	6.27%	5.36%
$\beta = 3.0$	3.09%	4.68%	11.21%	9.54%	8.07%	6.28%
$\beta = 3.5$	/	5.54%	6.97%	10.46%	7.94%	8.02%
$\beta = 4.0$	/	5.18%	6.73%	10.92%	9.19%	9.34%
Average	4.56%	6.98%	7.71%	6.78%	5.85%	5.58%
Total average				**6.25%**		

Table 2. Summary of the ultimate compressive reduction (NLFEM with residual stress in plate and stiffener web)

	$\lambda = 0.2$	$\lambda = 0.4$	$\lambda = 0.6$	$\lambda = 0.8$	$\lambda = 1.0$	$\lambda = 1.2$
$\beta = 1.0$	2.28%	10.03%	6.35%	5.20%	5.54%	2.41%
$\beta = 1.5$	8.39%	10.95%	9.77%	7.00%	4.48%	5.20%
$\beta = 2.0$	6.27%	9.37%	12.51%	10.35%	7.71%	5.57%
$\beta = 2.5$	4.41%	6.89%	13.79%	12.11%	10.51%	9.00%
$\beta = 3.0$	3.00%	4.86%	14.05%	14.00%	11.86%	9.91%
$\beta = 3.5$	/	6.39%	9.23%	14.87%	12.62%	11.66%
$\beta = 4.0$	/	5.88%	8.86%	15.55%	14.18%	12.95%
Average	4.87%	7.77%	10.65%	11.30%	9.56%	8.10%
Total average				**8.71%**		

Table 3. Summary of the ultimate compressive reduction (CSR-H with compressive yield strain = 2.0)

	$\lambda = 0.2$	$\lambda = 0.4$	$\lambda = 0.6$	$\lambda = 0.8$	$\lambda = 1.0$	$\lambda = 1.2$
$\beta = 1.0$	2.99%	5.96%	10.95%	12.54%	10.70%	7.77%
$\beta = 1.5$	12.81%	12.46%	11.79%	10.77%	9.18%	6.70%
$\beta = 2.0$	11.63%	11.19%	10.80%	9.93%	8.60%	6.60%
$\beta = 2.5$	11.15%	10.64%	10.14%	9.66%	8.50%	6.78%
$\beta = 3.0$	10.93%	10.33%	9.76%	9.49%	8.34%	6.65%
$\beta = 3.5$	10.86%	10.23%	9.60%	9.50%	8.62%	7.19%
$\beta = 4.0$	10.84%	10.16%	9.48%	9.00%	8.73%	7.37%
Average	10.17%	10.14%	10.36%	10.13%	8.95%	7.01%
Total average				**9.46%**		

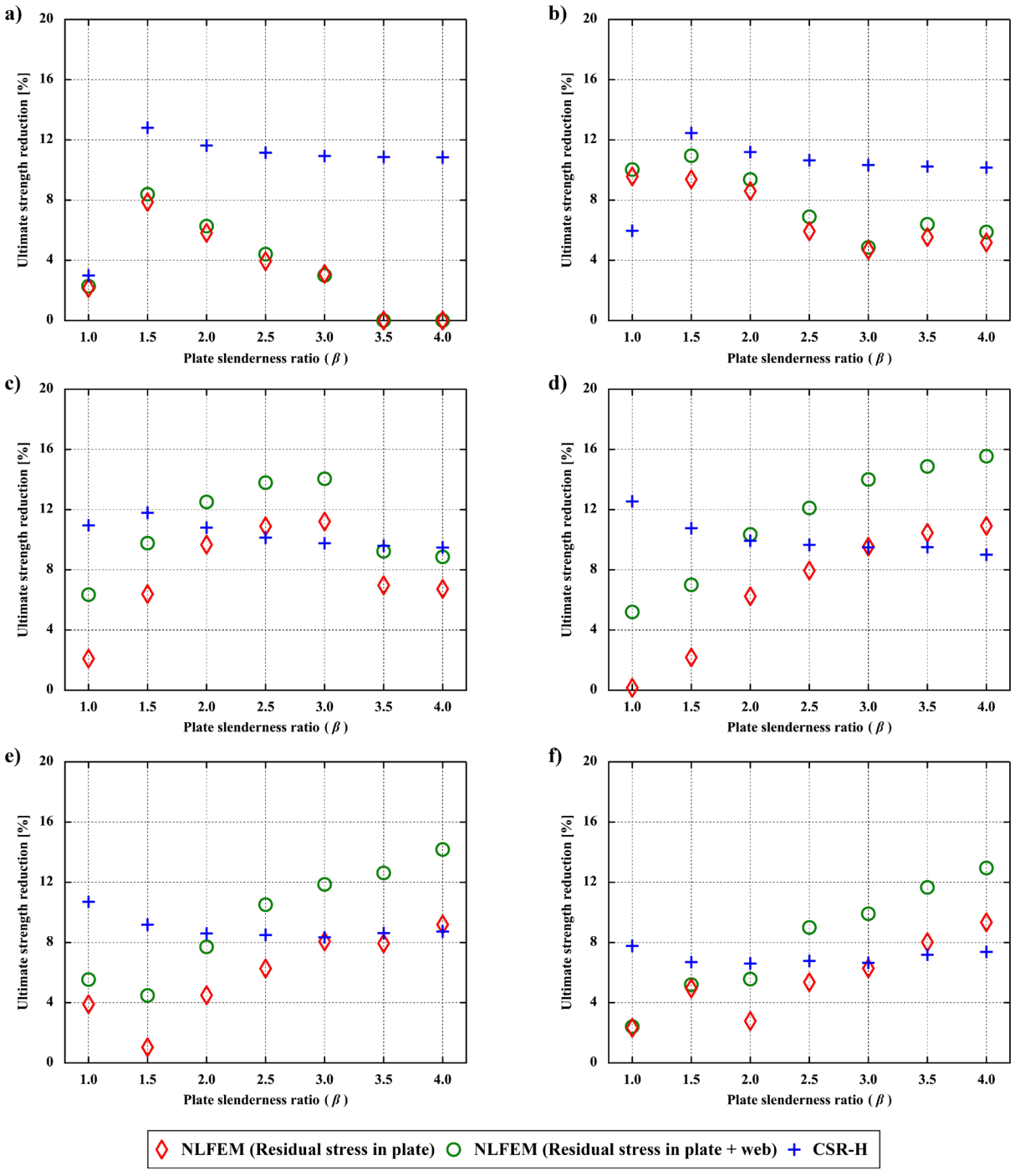

Figure 11. Comparison of ultimate compressive strength reduction; a) $\lambda = 0.2$; b) $\lambda = 0.4$; c) $\lambda = 0.6$; d) $\lambda = 0.8$; e) $\lambda = 1.0$; f) $\lambda = 1.2$

4. EXAMINATION OF THE MODIFIED EDGE FUNCTION APPROACH

The previous section compares the ultimate strength of stiffened panels predicted by NLFEM and IACS-CSR considering the effect of residual stress. It is shown that the CSR_H method with modified edge function approach may be conservative. In this section, a more detailed examination of the modified edge function approach is presented.

Two histograms are plotted in Figure 12 showing the distribution of the ratio between NLFEM and CSR-H prediction of ultimate compressive strength reduction. The mean values of two cases (i.e. residual stress in plate only and residual stress plate and web) are 0.67 and 0.94 respectively. However, the variance is considerably large with coefficients of deviation (COV) of 0.56 and 0.52 respectively. This comparison may indicate that the two methods are not statistically well-correlated, if the compressive yield strain equals to 2.0 in the modified edge function.

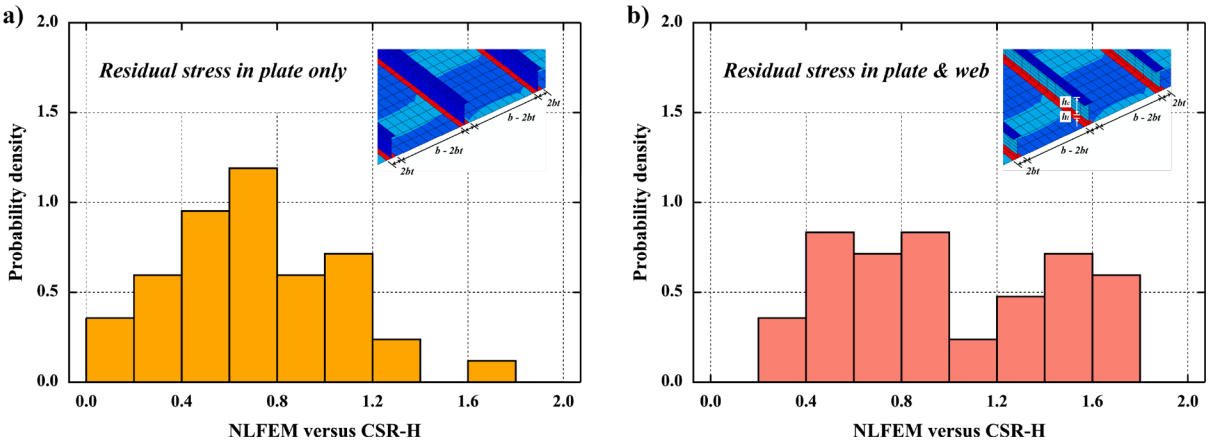

Figure 12. Histogram of the ratio between NLFEM and CSR-H prediction of strength reduction; a) residual stress in plate only; b) residual stress in plate and web

Nevertheless, the above comparison does not imply that the modified edge function approach is an incapable solution to deal with the effect of residual stress. As shown in Figure 13(a), a larger ultimate strength reduction can be predicted with an increase of the compressive yield strain. Note that when the compressive yield strain equals to unity, it corresponds to the initial stress-free condition and no reduction is shown. A better correlation may be obtained by changing the compressive yield strain. To determine the appropriate compressive yield strain of the tested panels, a series of computation are conducted by varying the compressive yield strain from 1.0 to 2.5 at an increment of 0.1, within which the best-correlated prediction with NLFEM results is selected to identify the appropriate compressive yield strain. However, since the ultimate reduction is not linearly increased with

compressive yield strain, which instead would converge to a certain value. With an increase of the compressive yield strain, the modified edge function effectively adapts the pre-collapse tangent stiffness as shown in Figure 13(b). Once the tangent stiffness is negative, the ultimate compressive strength is equal to the strength corresponding to the transition strain (i.e. $1.0 - \varepsilon_{rcx}/\varepsilon_{Yeq}$). A further modification will not lead to any additional strength reduction. Thus, even when compressive strain equals to 2.5, there is still a considerable deviation in some cases, which may suggest the limitation of the modified edge function approach. For these cases, the compressive yield strains are all taken 2.5 in the results illustrated in Figure 14.

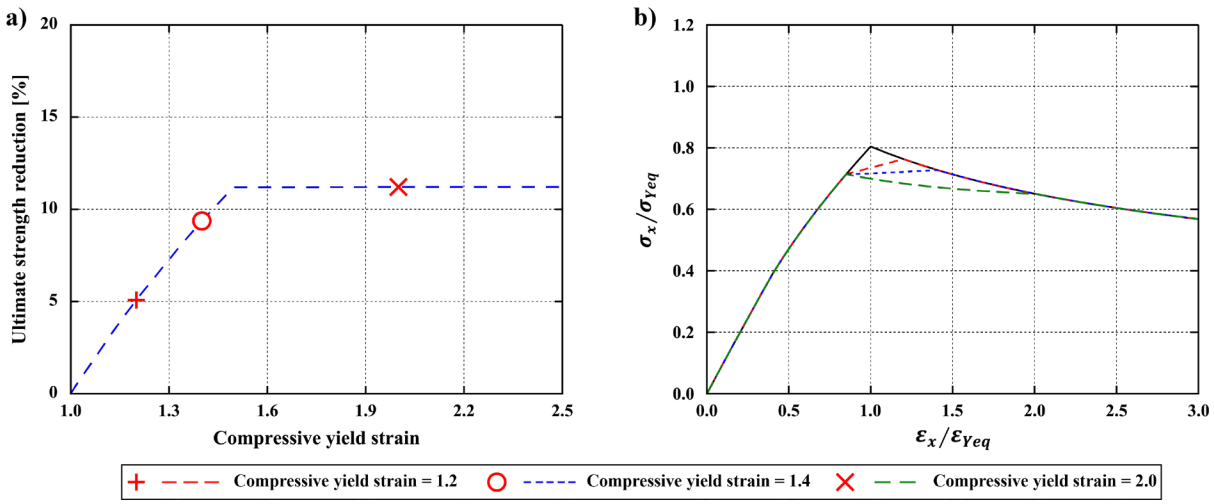

Figure 13. Example converging relation between compressive yield strain and ultimate strength reduction computed by the modified edge function approach ($\beta = 2.0, \lambda = 0.4$); a) convergence of the strength reduction; b) Corresponding load-shortening curves with different compressive yield strain.

It can be found from Figure 14 that in most cases the computed compressive yield strain is less than the provisional value of 2.0 originally suggested by Gordo and Guedes Soares [4]. For stiffened panels with $\lambda = 0.2$ and $\lambda = 0.4$, a suitable compressive yield strain can be computed to fit the NLFEM results of the two cases with residual stress. For more slender panels, a suitable compressive yield strain can only be computed to fit the NLFEM results with residual stress on plates. Conversely, a closely correlated result with the NLFEM results with residual stress on plates and webs cannot be obtained on slender stiffened panels even with a tremendous compressive yield strain. Following the sub-domain division introduced in section 3.3.1, these panels primarily correspond to the sub-domain 2 ($\beta > 1.9$ & $\lambda > 0.6$). However, as indicated by the survey by Zhang and Khan [63] on commercial ships, the most typical plate slenderness ratio and column slenderness ratio are in the range of $1.5 < \beta < 2.5$ and $0.2 <$

$\lambda < 0.8$. In this regard, the modified edge function approach can still be introduced as a practical method, but the provisional compressive yield strain of 2.0 should be revised. Future study is thus needed to calibrate the compressive yield strain.

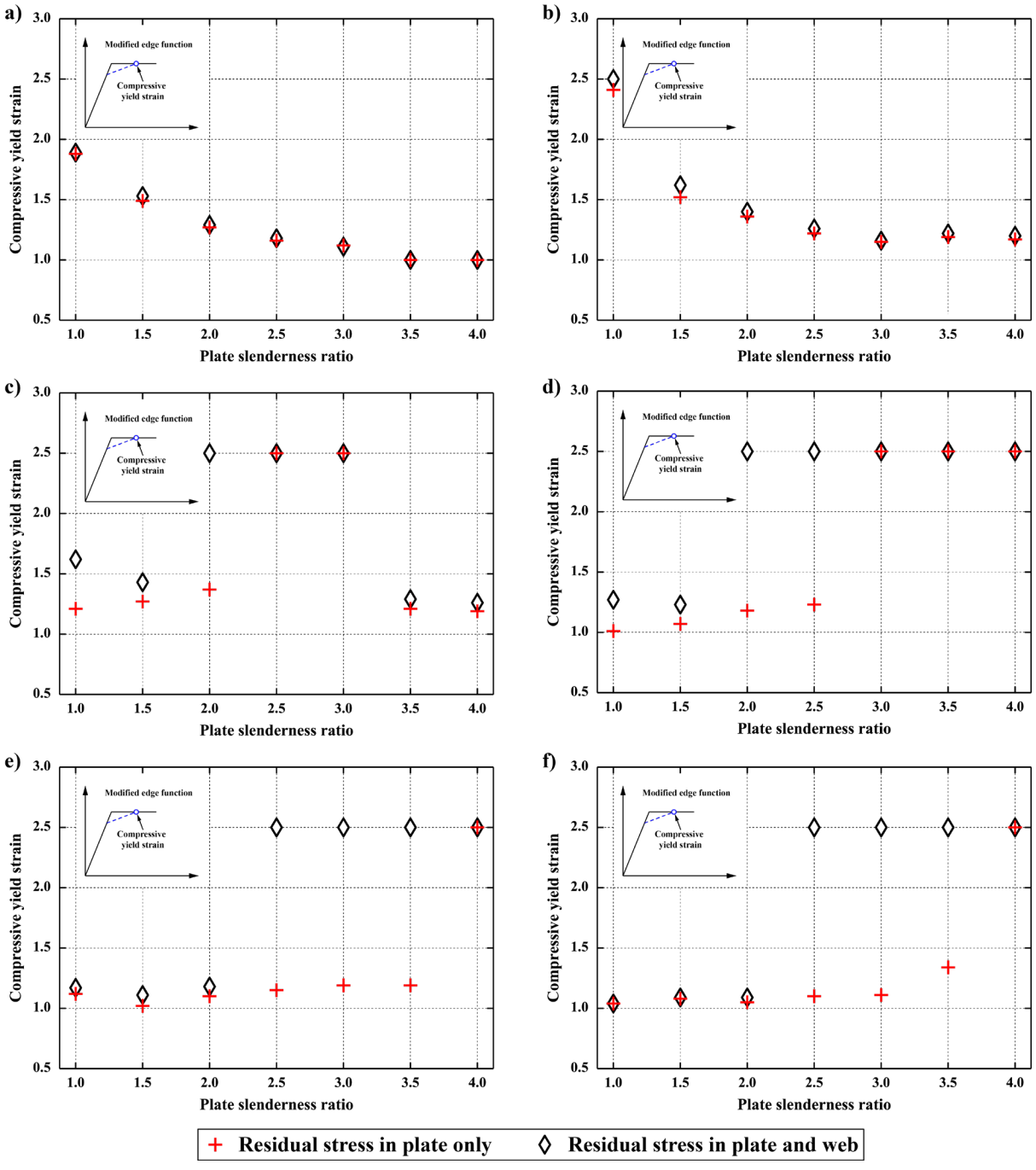

Figure 14. Computed compressive yield strain in the modified edge function approach; a) $\lambda = 0.2$; b) $\lambda = 0.4$; c) $\lambda = 0.6$; d) $\lambda = 0.8$; e) $\lambda = 1.0$; f) $\lambda = 1.2$

5. SENSITIVITY STUDY

A sensitivity study is presented in this section to elucidate the influence of alternative stiffener cross-sectional profiles and the impact of different residual stress magnitudes. For the former, angle-bar and flat-bar panels with $\beta = 2.0$ & $\lambda = 0.4$ and $\beta = 3.5$ & $\lambda = 0.8$ are analysed, which represents the stocky stiffened panels and slender stiffened panels respectively. The dimension of angle-bar stiffened panel is identical to the original tee-bar panel. The only difference is the change in cross-sectional profile. Conversely, with a ratio of $h_w/t_w = 10$ following Admiralty standard flat-bar section, the web of the flat-bar stiffened panel is scaled accordingly to keep the same column slenderness ratio. For the latter, two tee-bar stiffened panels are considered with $\beta = 2.0$ & $\lambda = 0.4$ and $\beta = 3.5$ & $\lambda = 0.8$ respectively. For both panels, three different levels of residual stress are analyses, following the Equation (4). In this sensitivity study, the residual stress is only on the local plating while the initial geometric imperfection is consistent with Equation (7) and (8).

5.1 Sensitivity to Stiffener Cross-Sectional Profiles

The computed ultimate strength of stiffened panels with alternative stiffener cross-sectional profiles is illustrated in Figure 15. It is clear that there is nearly no difference between the tee-bar and angle-bar stiffened panels regarding the strength reduction due to welding residual stress. In terms of the stocky flat-bar stiffened panels, the deviation is also negligible if the welding residual stress is applied only on the plating. When it comes to the slender flat-bar stiffened panel with welding residual stress on applied to plating, the strength reduction is smaller than the other panels. If the welding residual stress is applied to both plating and stiffener web, there is an increase of the strength reduction, in particular on the slender flat-bar panel. This is likely attributed to the open-section configuration of a flat-bar panel, which has a low torsional rigidity and hence would be more sensitive to any adverse factor related to the stiffeners. In general, it is suggested from this case study that the strength reduction due to welding residual stress is similar between flanged stiffened panels (tee-bar panels and angle-bar panels), whereas there could be a considerable uncertainty in stiffened panels with an open cross-section. Further research should be completed to elaborate on the investigation of the effects of welding residual stress on flat-bar stiffened panels.

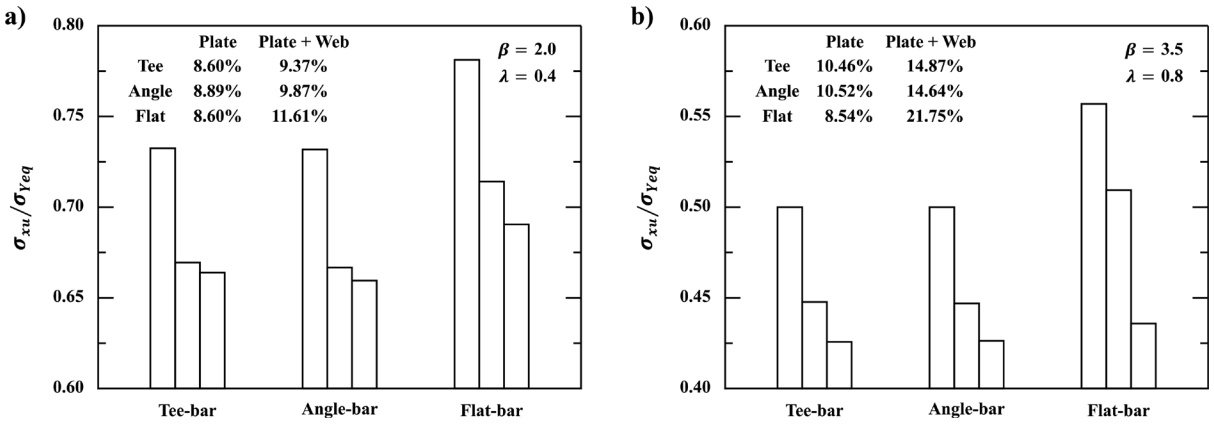

Figure 15. Comparison of the ultimate compressive strength of stiffened panels with various cross-sectional profiles

5.2 Sensitivity to Residual Stress Magnitudes

The comparison of the ultimate compressive strength of the case study stiffened panels with different residual stress magnitude is shown in Figure 16. In both cases, the strength reduction is increased with a greater residual stress magnitude, the pattern of which may be simplified as a linear relationship. The results presented in Figure 16 may be used to extrapolate the prediction summarised in Table 1 and Table 2 to evaluate the strength reduction due to different severities of welding residual stress.

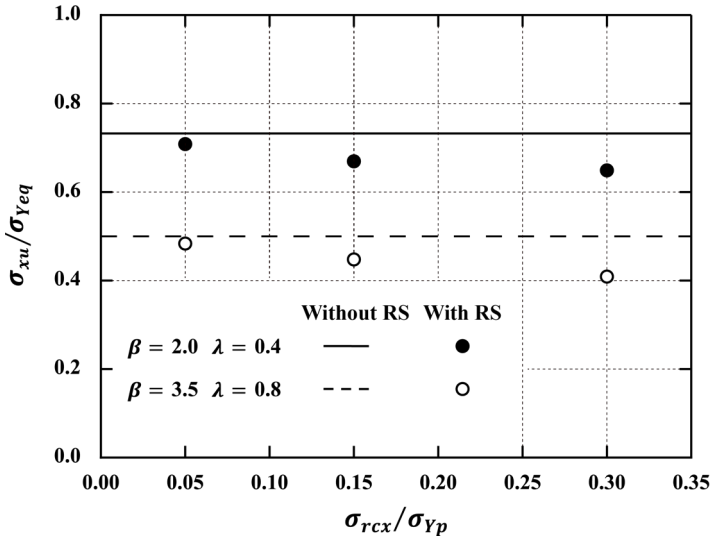

Figure 16. Comparison of the ultimate compressive strength of stiffened panels with different magnitudes of welding residual stress

6. DISCUSSION

As indicated in section 4, a calibration of the compressive yield strain used in the modified edge function approach should be conducted. This requires an extended test matrix covering different structural scantlings. The test matrix used in this study can be extended by considering different plate slenderness ratios, column slenderness ratio and area ratios. However, this should be confined to stiffened panels of sub-domains 1, 3 & 4, as the modified edge function approach may not be applicable for stiffened panels in sub-domain 2. In addition, different stiffener profiles might be included in the test matrix, such as angle-bar and flat-bar. There are also stiffened panels test matrix examples available in [64]. These test matrices are different from Smith's test matrix because of the difference in stiffener sizes. Therefore, even the two most common dimensionless parameters (plate slenderness ratio and column slenderness ratio) are the same, the behaviour of stiffened panel can differ due to uncertainty caused by different stiffness ratio or web height to thickness ratio etc. The data based on a wider spectrum of analyses could thus be more representative. Once a sufficient number of data is collected, the calibration can be conducted using a simple response surface method or multivariable polynomial response surface regression [78-79]. In addition, more sophisticated neural network methods, which is part of the deep learning technique [80-83], could be applied to resolve complicated engineering issues..

Similarly, formulae for predicting ultimate compressive strength reduction can be developed. Although a calibrated compressive yield strain in combination with the CSR-H method is able to predict the ultimate compressive strength reduction, a more efficient closed-form formula would be useful. In addition, this formula may be able to cover a wider range of stiffened panels, since the modified edge function approach may have limitations.

7. CONCLUSIONS

A parametric numerical collapse test is conducted using the nonlinear finite element method to evaluate the effects of welding-induced residual stress on the ultimate compressive strength of a typical range of stiffened panels. Comparison is made with the CSR-H method combined with the modified edge function. From this study, the following conclusions may be drawn:

- The welding-induced residual stress with average severity will significantly reduce the ultimate compressive strength of most stiffened panels under testing. However, the detrimental influence on the strength of stiffened panels, with a combination of low plate slenderness and high column slenderness or with a combination of high plate slenderness and low column slenderness, is marginal;

- According to the NLFEM results, if the residual stress is only considered in the local plate, the mean reduction is approximately 6%. If the residual stress is considered in both local plate and stiffener, the mean reduction is close to 8.5%. However, considerable deviations exist in these measures due to the difference in structural scantlings and failure modes between tested panels;
- With the provisional compressive yield strain originally suggested by Gordo and Guedes Soares [4], the modified edge function approach is not statistically well-correlated with the NLFEM results, with a coefficient of deviation of more than 50%;
- The modified edge function is also challenged by the fact that it may not be applicable for slender stiffened panels, due to the converging relationship between compressive yield strain and strength reduction;
- Nevertheless, the modified edge function approach is still a practical method, at least for merchant ship structures if an appropriate compressive yield strain is determined. This may be completed in a future numerical study with an extended test cases but limited range of plate slenderness ratio and column slenderness ratio. With a sufficient dataset, advanced data processing techniques can be adopted to derive an empirical formulation.

REFERENCES

[1] Gannon, L., Liu, Y., Pegg, N., Smith, M.J., 2016. Nonlinear collapse analysis of stiffened plates considering welding-induced residual stress and distortion. Ships and Offshore Structures, 11, 228–244.

[2] Gannon, L., Liu, Y., Pegg, N., Smith, M.J., 2013. Effect of three-dimensional welding-induced residual stress and distortion fields on strength and behaviour of flat-bar stiffened panels. Ships and Offshore Structures, 8(5), 565-578.

[3] Hansen, A.M., 1996. Strength of midship sections. Marine Structures, 9, 471–494.

[4] Gordo, J.M., Guedes Soares, C., 1993. Approximate load shortening curves for stiffened plates under uniaxial compression. In: Integrity of Offshore Structures (Faulkner et al, Eds.), UK.

[5] Khan I, Zhang SM, 2011. Effects of welding-induced residual stress on ultimate strength of plates and stiffened panels. Ships and Offshore Structures, 6, 297–309.

[6] Gannon, L., Liu, Y., Pegg, N., Smith, M.J., 2012. Effect of welding-induced residual stress and distortion on ship hull girder ultimate strength. Marine Structures, 28, 25–49.

[7] Gordo, J.M., 2020. Effect of residual stresses on the elastoplastic behavior of welded steel plates. Journal of Marine Science and Engineering, 8(9), 702.

[8] IACS, 2019. Common Structural Rules for Bulk Carriers and Oil Tankers.

[9] IACS, 2015. Longitudinal Strength Standard for Container Ships.

[10] Li, S., Benson, S., 2020. The effects of welding-induced residual stress on the buckling collapse behaviours of stiffened panels. In: 5th International Conference on Maritime Technology and Engineering, Lisbon, Portugal.

[11] Benson, S., Downes, J., Dow, R.S., 2013. Compartment level progressive collapse analysis of lightweight ship structures. Marine Structures, 31, 44-62.

[12] Li, S., Hu, Z., Benson, S., 2020. Progressive collapse analysis of ship hull girders subjected to extreme cyclic bending. Marine Structures, 73, 102803.

[13] Li, S., Hu, Z., Benson, S., 2019. An analytical method to predict the buckling and collapse behaviour of plates and stiffened panels under cyclic loading. Engineering Structures, 199, 109627.

[14] Benson, S., Downes, J., Dow, R.S., 2015. Overall buckling of lightweight stiffened panels using an adapted orthotropic plate method. Engineering Structures, 85, 107-117.

[15] Smith, C.S., Davidson, P.C., Chapman, J.C., Dowling, P.J., 1987. Strength and stiffness of ships' plating under in-plane compression and tension. Transaction of RINA, 130, 277–293.

[16] Smith, C.S., Anderson, N., Chapman, J.C., Davidson, P.J., Dowling, P.J., 1991. Strength of stiffened plating under combined compression and lateral pressure. Transactions of Royal Institution of Naval Architects, 131–147.

[17] Benson, S., Downes, J., Dow, R.S., 2011. Ultimate strength characteristics of aluminium plates for high-speed vessels. Ships and Offshore Structures, 6, 67-80.

[18] Benson, S., Downes, J., Dow, R.S., 2013. Load shortening characteristics of marine grade aluminium alloy plates in longitudinal compression. Thin-Walled Structures, 70, 19-32.

[19] Tanaka, S., Yanagihara, D., Yasuoka, A., Harada, M., Okazawa, S., Fujikubo, M., Yao, T., 2014. Evaluation of ultimate strength of stiffened panels under longitudinal thrust. Marine Structures, 36, 21-50

[20] Gordo, J.M., 2015. Effect of initial imperfections on the strength of restrained plates. Journal of Offshore Mechanics and Arctic Engineering, 137(5), 051401.

[21] Paik, J.K., Thayamballi, A., Lee, J.M., 2004. Effect of initial deflection shape on the ultimate strength behavior of welded steel plates under biaxial compressive loads. Journal of Ship Research, 48(1), 45-60.

[22] Xu, M.C., Yanagihara, D., Fujikubo, M., Guedes Soares, C., 2013. Influence of boundary conditions on the collapse behaviour of stiffened panels under combined loads. Marine Structures, 34, 205-255.

[23] Syrigou, M., Benson, S., Dow, R.S., 2015. Strength of aluminium alloy ship plating under combined shear and compression/tension. Analysis and Design of Marine Structures V, 487-496.

[24] Syrigou, M., Dow, R.S., 2018. Strength of steel and aluminium alloy ship plating under combined shear and compression/tension. Engineering Structures, 166, 128-141.

[25] Zhang, S., Kumar, P., Rutherford, S.E., 2008. Ultimate shear strength of plates and stiffened panels. Ships and Offshore Structures, 3, 105-112.

[26] Li, S., Benson, S., 2019. A re-evaluation of the hull girder shakedown limit states. Ships and Offshore Structures, 14:sup1, 239-250.

[27] Zhang, X., Paik, J.K., Jones, N., 2015. A new method for assessing the shakedown limit state associated with the breakage of a ship's hull girder. Ships and Offshore Structure, 11(1), 92–104.

[28] Li, S., Hu, Z., Benson, S., 2019. Bending response of a damaged ship hull girder predicted by the cyclic progressive collapse method. In Proceeding: International Conference on Collision and Grounding of Ships and Offshore Structures (ICCGS), Lisbon, Portugal.

[29] Paik, J.K., Lee, D.H., Noh, S.H., Park, D.K., Ringsberg, J.W., 2020. Full-scale collapse testing of a steel stiffened plate structure under cyclic compressive loading. Structures, 26, 996-1009.

[30] Liu, B., Guedes Soares, C., 2020. Ultimate strength assessment of ship hull structures subjected to cyclic bending moments. Ocean Engineering, 215, 107685.

[31] Tekgoz, M., Garbatov, Y., 2020. Strength assessment of rectangular plates subjected to extreme cyclic load reversals. Journal of Marine Science and Engineering 8(2), 65.

[32] Ehlers, S., Benson, S., Misirlis, K., 2013. Ultimate strength of an intact and damaged LNG vessel subjected to sub-zero temperature. In Proceeding: 6th International Conference on Collision and Grounding of Ship and Offshore Structures (ICCGS), Trondheim, Norway.

[33] Kim, D.K., Kim, H.B., Park, D.H., Mohd, M.H., Paik, J.K., 2020. A practical diagram to determine the residual longitudinal strength of grounded ship in Northern Sea Route. Ships and Offshore Structures, 15, 683-700.

[34] Park, D.K., Kim, D.K., Seo, J.K., Kim, B.J., Ha, Y.C., Paik, J.K., 2015. Operability of non-ice class aged ships in the Arctic Ocean - Part I: Ultimate limit state approach. Ocean Engineering, 102, 197-205.

[35] Paik, J.K., Lee, D.H., Park D.K., Ringsberg, J.W., 2020. Full-scale collapse testing of a steel stiffened plate structure under axial-compressive loading at a temperature of −80°C. Ships and Offshore Structures, In-press (https://doi.org/10.1080/17445302.2020.1791685).

[36] Paik, J.K., Lee, D.H., Noh, S.H., Park D.K., Ringsberg, J.W., 2020. Full-scale collapse testing of a steel stiffened plate structure under axial-compressive loading triggered by brittle fracture at cryogenic condition, Ships and Offshore Structures, In-press (http://doi.org/10.1080/17445302.2020.1787930).

[37] Fanourgakis, S.D., Samuelides, M., 2020. Study of hull girder ultimate strength at elevated temperatures. In: 5th International Conference on Ships and Offshore Structures. Glasgow, UK.

[38] Kim, D.K., Liew, M.S., Youssef, S.A.M., Mohd, M.H., Kim, H.B., Paik, J.K., 2014. Time-dependent ultimate strength performance of corroded FPSOs. Arabian Journal for Science and Engineering, 39, 7673-7690.

[39] Kim, D.K., Kim, S.J., Kim, H.B., Zhang, X.M., Li, C.G., Paik, J.K., 2015. Ultimate strength performance of bulk carriers with various corrosion additions. Ships and Offshore Structures, 10, 59-78.

[40] Wang, Y., Downes, J., Wharton, J., Shenoi, R., 2018. Assessing the performances of elastic-plastic buckling and shell-solid combination in finite element analysis on plated structures with and without idealised corrosion defects. Thin-Walled Structures, 127, 17-30.

[41] Wang, Y., Wharton, J., Shenoi, A., 2016. Mechano-electrochemical modelling of corroded steel structures. Engineering Structures, 128, 1-14.

[42] Wang, Y., Wharton, J. A., Shenoi, A., 2015. Ultimate strength assessment of steel stiffened plate structures with grooving corrosion damage. Engineering Structures, 94, 29-42.

[43] Wang, Y., Wharton, J. A., & Shenoi, R. A., 2014. Influence of localized pit distribution and bench-shaped pits on the ultimate compressive strength of steel plating for shipping. Corrosion, 70(9), 915-927

[44] Wang, F., Paik, J.K., Kim, B.J., Cui, W.C., Hayat, T., Ahmad, B., 2015. Ultimate shear strength of intact and cracked stiffened panels. Thin-Walled Structures, 88, 48-57.

[45] Leelachai, A., Benson, S.D., Dow, R.S., 2015. Progressive collapse of intact and damaged stiffened panels. In Proceeding: 5th International Conference on Marine Structures (MARSTRUCT), Southampton, United Kingdom.

[46] Benson, S., AbuBakar, A., Dow, R.S., 2013. A comparison of computational methods to predict the progressive collapse behaviour of a damaged box girder. Engineering Structures, 48, 266-280.

[47] Benson, S., Syrigou, M., Dow, R.S., 2013. Longitudinal strength assessment of damaged box girders. In Proceeding: 6th International Conference on Collision and Grounding of Ship and Offshore Structures (ICCGS), Trondheim, Norway.

[48] Li, S., Hu, Z., Benson, S., 2020. Ultimate strength performance of a damaged container ship. International Conference on Damaged Ship, RINA, London, UK.

[49] Kim, D.K., Pedersen, P.T., Paik, J.K., Kim, H.B., Zhang, X.M., Kim, M.S., 2013. Safety guidelines of ultimate hull girder strength for grounded container ships, 59, 46-54.

[50] Cerik, B.C., Cho, S.R., 2013. Numerical investigation on the ultimate strength of stiffened cylindrical shells considering residual stresses and shakedown. Journal of Marine Science and Technology, 18, 524-534.

[51] Gannon, L.G., Pegg, N.G., Smith M.J., Liu, Y., 2013. Effect of residual stress shakedown on stiffened plate strength and behaviour. Ships and Offshore Structures, 8(6), 638-652

[52] Yao, T., Fujikubo, M., 2016. Buckling and ultimate strength of ship and ship-like floating structures, Elsevier.

[53] Tekgoz, M., Garbotov, Y., Guedes Soares, C., 2015. Ultimate strength assessment of welded stiffened plates. Engineering Structures, 84(1), 325-339.

[54] Paik, J.K., Thayamballi, A.K., 2003. Ultimate limit state design of steel-plated structures, John Wiley & Sons, Chichester, UK.

[55] Yi, M.S., Noha, S.H., Lee, D.H., Seo, D.H., Paik, J.K., 2020. Direct measurements, numerical predictions and simple formula estimations of welding-induced biaxial residual stresses in a full-scale steel stiffened plate structure. Structures (In press).

[56] Yi, M.S., Hyun, C.M., Paik, J.K., 2018. Three-dimensional thermo-elastic-plastic finite element method modeling for predicting weld-induced residual stresses and distortions in steel stiffened-plate structures. World Journal of Engineering and Technology, 6, 176-200.

[57] Yi, M.S., Hyun, C.M., Paik, J.K., 2018. Full-scale measurements of welding-induced initial deflections and residual stresses in steel-stiffened plate structures. International Journal Maritime Engineering , 160 (A4) , Article 504.

[58] Chen and Guedes Soares, 2021. Experimental and numerical investigation on welding simulation of long stiffened steel plate specimen. Marine Structures, 75, 102824.

[59] Yao, T., 1980. Compressive ultimate strength of structural members in ship structure. PhD thesis, Osaka University, Japan (in Japanese).

[60] Yi, M.S., Hyun, C.M., Paik, J.K., 2019. An empirical formulation for predicting welding-induced biaxial compressive residual stresses on steel stiffened plate structures and its application to thermal plate buckling prevention. Ships and Offshore Structures, 14: sup1, 18-33.

[61] Chalmers, D.W., 1993. Design of Ship's Structures. London: HMSO.

[62] Dow, R.S., 1997. Structural redundancy and damage tolerance in relation to ultimate ship hull strength. In Proceeding: Advances in Marine Structures 3, DERA, Dunfermline, Scotland.

[63] Zhang, S., Khan, I., 2009. Buckling and ultimate capability of plates and stiffened panels in axial compression. Marine Structures, 22, 791–808.

[64] ISSC, 2012. Ultimate Strength (Committee III.1). The 18th International Ship and Offshore Structures Congress (ISSC 2012). 9-13 September, Rostock, Germany.

[65] Smith, M.J., 2010. A load shortening curve library for longitudinally stiffened panels. Technical Memorandum, DRDC Atlantic.

[66] Dowling, P.J., Chatterjee, S., Frieze, P.A., 1973. Experimental and predicted collapse behaviour of rectangular steel box girders. In: International Conference on Steel Box Girder Bridges, London.

[67] Antoniou, A.C., 1980. On the maximum deflection of plating in newly built ships. Journal of ship research, 24.

[68] Kmiecik, M., 1981. Factors affecting the load-carrying capacity of plates. Technical University of Szczecin, Ship Research Institution, Report No. 115.

[69] Carlsen, C.A., Czujko, J., 1978. The specification of post-welding distortion tolerances for stiffened plates in compression. The Structural Engineer, 54A, 133-141.

[70] Merrison Committee, 1973. Inquiry into the basis of design and method of erection of steel box bridges, Appendix I (Interim Design and Workmanship Rules). HMSO, London.

[71] Benson, S., Downes, J., Dow, R.S., 2012. An automated finite element methodology for hull girder progressive collapse analysis. In: 13th International Marine Design Conference, Glasgow, Scotland.

[72] Paik, J.K., Thayamballi, A.K., 1997. An empirical formulation for predicting the ultimate compressive strength of stiffened panels. In: 7th International Offshore and Polar Engineering Conference (ISOPE 1997), 25-30 May, Honolulu, Hawaii, USA (ISOPE-I-97-444).

[73] Kim, D.K., Lim, H.L., Kim, M.S., Hwang, O.J., Park, K.S., 2017. An empirical formulation for predicting the ultimate strength of stiffened panels subjected to longitudinal compression. Ocean Engineering, 140, 270–280.

[74] Zhang, S.M., 2016. A review and study on ultimate strength of steel plates and stiffened panels in axial compression. Ships and Offshore Structures, 11, 81–91.

[75] Kim, D.K., Lim, H.L., Yu, S.Y., 2018. A technical review on ultimate strength prediction of stiffened panels in axial compression. Ocean Engineering, 170, 392-406.

[76] Li, S., Kim, D.K., Benson, S., 2020. An adaptable algorithm to predict the load-shortening curves of stiffened panels in longitudinal compression. Ships and Offshore Structures (Under review).

[77] Ozdemir M., Ergin A., Yanagihara D., Tanaka S., Yao T. 2018. A new method to estimate ultimate strength of stiffened panels under longitudinal thrust based on analytical formulas. Marine Structures, 59, 510–535.

[78] Kim, D.K., Lim, H.L., Yu, S.Y., 2019. Ultimate strength prediction of T-bar stiffened panel under longitudinal compression by data processing: A refined empirical formulation. Ocean Engineering, 192, 106522.

[79] Kim, D.K., Yu, S.Y., Lim, H.L., Cho, N.K., 2020. Ultimate Compressive Strength of Stiffened Panel: An Empirical Formulation for Flat-Bar Type. Journal of Marine Science and Engineering, 8, 605.

[80] Wong, E.W.C., Kim, D.K., 2018. A simplified method to predict fatigue damage of TTR subjected to shortterm VIV using artificial neural network. Advances in Engineering Software, 126, 100-109.

[81] Pu, Y., Mesbahi, E., 2006. Application of artificial neural networks to evaluation of ultimate strength of steel panels. Engineering Structures, 28, 1190-1196.

[82] Ahmadi, F., Ranji, A.R., Nowruzi, H. 2020. Ultimate strength prediction of corroded plates with center-longitudinal crack using FEM and ANN. Ocean Engineering, 206, 107281.

[83] Ok, D., Pu, Y., Incecik, A. 2007. Artificial neural networks and their application to assessment of ultimate strength of plates with pitting corrosion. Ocean Engineering, 34, 2222-2230.

APPENDIX

Table A1. Summary of the tested stiffened panels

a	b	t_p	h_w	t_w	b_f	t_f	β	λ	γ
593.7	311.1	12.3	104.8	5.1	44.5	9.5	1.0	0.2	0.2
1187.4	311.1	12.3	104.8	5.1	44.5	9.5	1.0	0.4	0.2
1781.1	311.1	12.3	104.8	5.1	44.5	9.5	1.0	0.6	0.2
2374.8	311.1	12.3	104.8	5.1	44.5	9.5	1.0	0.8	0.2
2968.5	311.1	12.3	104.8	5.1	44.5	9.5	1.0	1.0	0.2
3562.2	311.1	12.3	104.8	5.1	44.5	9.5	1.0	1.2	0.2
586.5	381.0	10.0	104.8	5.1	44.5	9.5	1.5	0.2	0.2
1173.1	381.0	10.0	104.8	5.1	44.5	9.5	1.5	0.4	0.2
1759.6	381.0	10.0	104.8	5.1	44.5	9.5	1.5	0.6	0.2
2346.2	381.0	10.0	104.8	5.1	44.5	9.5	1.5	0.8	0.2
2932.7	381.0	10.0	104.8	5.1	44.5	9.5	1.5	1.0	0.2
3519.3	381.0	10.0	104.8	5.1	44.5	9.5	1.5	1.2	0.2
582.4	440.0	8.7	104.8	5.1	44.5	9.5	2.0	0.2	0.2
1164.7	440.0	8.7	104.8	5.1	44.5	9.5	2.0	0.4	0.2
1747.1	440.0	8.7	104.8	5.1	44.5	9.5	2.0	0.6	0.2
2329.4	440.0	8.7	104.8	5.1	44.5	9.5	2.0	0.8	0.2
2911.8	440.0	8.7	104.8	5.1	44.5	9.5	2.0	1.0	0.2
3494.1	440.0	8.7	104.8	5.1	44.5	9.5	2.0	1.2	0.2
579.5	491.9	7.8	104.8	5.1	44.5	9.5	2.5	0.2	0.2
1159.1	491.9	7.8	104.8	5.1	44.5	9.5	2.5	0.4	0.2
1738.6	491.9	7.8	104.8	5.1	44.5	9.5	2.5	0.6	0.2
2318.1	491.9	7.8	104.8	5.1	44.5	9.5	2.5	0.8	0.2
2897.6	491.9	7.8	104.8	5.1	44.5	9.5	2.5	1.0	0.2
3477.2	491.9	7.8	104.8	5.1	44.5	9.5	2.5	1.2	0.2
594.1	538.8	7.1	104.8	5.1	44.5	9.5	3.0	0.2	0.2
1188.3	538.8	7.1	104.8	5.1	44.5	9.5	3.0	0.4	0.2
1782.4	538.8	7.1	104.8	5.1	44.5	9.5	3.0	0.6	0.2
2376.6	538.8	7.1	104.8	5.1	44.5	9.5	3.0	0.8	0.2
2970.7	538.8	7.1	104.8	5.1	44.5	9.5	3.0	1.0	0.2
3564.9	538.8	7.1	104.8	5.1	44.5	9.5	3.0	1.2	0.2
575.9	582.0	6.6	104.8	5.1	44.5	9.5	3.5	0.2	0.2
1151.7	582.0	6.6	104.8	5.1	44.5	9.5	3.5	0.4	0.2
1727.6	582.0	6.6	104.8	5.1	44.5	9.5	3.5	0.6	0.2
2303.4	582.0	6.6	104.8	5.1	44.5	9.5	3.5	0.8	0.2
2879.3	582.0	6.6	104.8	5.1	44.5	9.5	3.5	1.0	0.2
3455.2	582.0	6.6	104.8	5.1	44.5	9.5	3.5	1.2	0.2
574.6	622.2	6.2	104.8	5.1	44.5	9.5	4.0	0.2	0.2
1149.2	622.2	6.2	104.8	5.1	44.5	9.5	4.0	0.4	0.2
1723.7	622.2	6.2	104.8	5.1	44.5	9.5	4.0	0.6	0.2
2298.3	622.2	6.2	104.8	5.1	44.5	9.5	4.0	0.8	0.2
2872.9	622.2	6.2	104.8	5.1	44.5	9.5	4.0	1.0	0.2
3447.5	622.2	6.2	104.8	5.1	44.5	9.5	4.0	1.2	0.2